Journal of Solid State Chemistry 182 (2009) 2930–2936

Contents lists available at ScienceDirect

Journal of Solid State Chemistry

journal homepage: www.elsevier.com/locate/jssc

Giant dielectric constant response of the composites in ternary system $CuO–TiO_2–CaO$

Michael Veith*, Shuhua Ren, Matthias Wittmar, Henning Bolz

INM – Leibniz Institute for New Materials, Campus D2 2, 66123 Saarbruecken, Germany

ARTICLE INFO

Article history:
Received 29 April 2009
Received in revised form
28 July 2009
Accepted 4 August 2009
Available online 8 August 2009

Keywords:
Cu–Ti–Ca–O system
Phase relations
Dielectric properties
Microstructure

ABSTRACT

The subsolidus phase relations of the ternary system $CuO–TiO_2–CaO$ sintered at 950 °C in air have been determined by powder X-ray diffraction method. Only one ternary compound $CaCu_3Ti_4O_{12}$ was found in this system. From room-temperature dielectric property mapping at 10 kHz, a giant dielectric constant ($\varepsilon_r > 10^4$) was observed for most of the ceramic composites in the CuO-rich region and in the region along the CaO–CuO binary line. The composites in the $CaCu_3Ti_4O_{12}$-rich region were found to give a comparable giant dielectric constant when sintered at 1050 °C. The particular microstructure of larger grains with predominant phase surrounded by smaller grains with the secondary phases was found in such composites with a high dielectric constant. The relations between structures and dielectric properties were investigated. An internal barrier layer capacitance effect is the most probable mechanism to explain this particular dielectric behavior.

1. Introduction

Materials with high dielectric constants (ε_r) accompanied by low dielectric loss ($\tan\delta$) and good temperature stability are very desirable due to their significant applications in microelectronic devices such as capacitors and memory devices [1,2]. Although ferroelectric materials such as Ba/Pb-based perovskite oxides have been widely used, the strong variation of the ε_r with temperature in these materials often limits their application. Furthermore, Ba/Pb-free ceramic capacitors are needed to meet the requirements of environmentally friendly materials [3].

Subramanian et al. [1] discovered that $CaCu_3Ti_4O_{12}$ possesses a giant ε_r of 10^4, which is nearly constant below 1 MHz over a wide temperature range from −173 to 327 °C [4]. A similar promising dielectric behavior was also found in CuO [5]. Though the origin of such dielectric behavior is still unknown, an internal barrier layer capacitor is generally considered as the most probable mechanism [5–7]. Also, (Ca, Ta)-doped TiO_2 ceramics show ultrahigh $\varepsilon_r > 10^4$, and a grain-boundary atomic defect model was proposed to explain such a behavior [8]. Kobayashi et al. [3] investigated the dielectric properties of two-phase composites of $CaCu_3Ti_4O_{12}$ and $CaTiO_3$. A high ε_r (≈ 1800) with a low $\tan\delta$ (≤ 0.02) below 100 kHz was obtained at $CaCu_3Ti_4O_{12}$:$CaTiO_3$ ratio of 2:1. A barrier layer of $CaTiO_3$ on the surface of the $CaCu_3Ti_4O_{12}$ grains was proposed to be the possible contribution to the high dielectric performance.

Based on the above-mentioned investigations, the particular observations in $CaCu_3Ti_4O_{12}$, CuO, etc. make the ternary system $CuO–TiO_2–CaO$ a potentially interesting system for dielectric property investigations. The phase diagrams of binary systems of CaO–CuO [9–11], $CaO–TiO_2$ [12,13], $CuO–TiO_2$ [14,15] have been previously studied by others. Very recently, Jacob et al. computed the phase diagram for the system $CaO–TiO_2–CuO/Cu_2O$ at 1000 °C as a function of oxygen partial pressure [16]. No experimental phase relationship investigation in ternary system $CuO–TiO_2–CaO$ has been done. The composition and the structure of phases within the $CuO–TiO_2–CaO$ system should play an important role in the dielectric properties. Therefore, it seemed to be quite promising to investigate the phases and their dielectric properties of the composites in the ternary system $CuO–TiO_2–CaO$ systematically.

In the present study, the subsolidus phase relationship and the dielectric properties in $CuO–TiO_2–CaO$ system were investigated. Parallel synthesis by an injection molding technique developed in our group was applied [17]. To avoid a liquid phase, all the samples were investigated after sintering at 950 °C. Some samples near the $CaCu_3Ti_4O_{12}$ region were also synthesized by sintering at 1050 °C. The composites in CuO-rich region and along CaO–CuO binary line were found to show a giant ε_r ($>10^4$) at a sintering temperature of only 950 °C. The composites in $CaCu_3Ti_4O_{12}$-rich region gave large $\varepsilon_r \approx 10^4$ when sintered at 1050 °C. The internal barrier layer capacitance effect might give an important contribution to the dielectric properties of the composites. The main objective of this work is to provide the experimental evidence between the multiphase microstructure and the dielectric response in the ternary system $CuO–TiO_2–CaO$.

* Corresponding author. Fax: +49 681 9300 223.
E-mail address: Michael.Veith@inm-gmbh.de (M. Veith).

0022-4596/$ - see front matter © 2009 Elsevier Inc. All rights reserved.
doi:10.1016/j.jssc.2009.08.006

2. Experimental

The preparation of the composites in the whole system was based on combinatorial parallel synthesis from injection molding [17]. $CaCO_3$ (SOCAL® 312, Solvay Chemicals), CuO (Nanostructured & Amorphous Materials Inc.), and TiO_2 (P25, Degussa) powders were used. The well-mixed low-viscosity feedstocks made of powder and the wax-based binder were shaped into triangular pyramid layer geometry by injection molding. The binder was a mixture of paraffin wax (Terhell@ Typ 5405, Schömann) and Luwax V (BASF) by weight ratio of 2.3:1.0. The weight ratio of the powder to binder is ca. 3.3:1.0. Additionally, 3.5 wt% of stearic acid was added as surfactant for TiO_2 powder. Three injected layers composed of CuO, TiO_2, or $CaCO_3$ feedstock, respectively, were stacked on top of one another to form a triangular prism, and cut vertically by an aluminum honeycomb (cell size: 6.4 mm). The schematic set-up of the above process was published elsewhere [17]. Each individual-layered piece inside the honeycomb was manually transferred to an aluminum rack with 70 parallel wells. Dilution agents such as decane and paraffin wax were added into each well (diameter: ~10 mm, depth: ~30 mm). Dielectric properties are very sensitive to variation of the microstructure. In order to get a more homogeneous mixture, a stainless steel ball (diameter: 6 mm) was put into each well of the aluminum rack to help the mixing. The covered rack was shaken in a red-devil painter mixer (Chameleon M & T Machines Ltd.) at 120 °C for 0.5 h, and then cooled during shaking. After removal of the stainless steel balls, all mixtures were individually transferred to alumina crucibles and calcined in air at 900 °C for 6 h, followed by grinding in an agate mortar. This process was repeated four more times to improve the homogeneity of the mixing. The as-obtained powder was pressed into pellets of 5 mm in diameter and 1.2–1.5 mm in thickness under 5 kN, followed by isostatical pressing under 2000 kN. The pellets were sintered at 950 °C (some at 1050 °C) for 70 h, followed by cooling in the furnace.

Each composition in this library depends on its geometrical position in the honeycomb, the content of metal oxide in each layer, and the molecular weight of the components. The composition in molar fraction of each composite was accordingly calculated [17]. A total of 171 compositions were achieved in this library.

X-ray powder diffraction patterns were recorded with a Siemens D-500 diffractometer equipped with a graphite monochromator using Cu $K\alpha$ radiation ($\lambda = 1.54178$ Å) in the range from 15 to 65° in 2θ and a counting time of 4 s/step. The relatively long scan times were used, especially when the sample was close to phase boundaries. An SEM instrument equipped with energy-dispersive X-ray spectroscopy (EDX) was used to observe the microstructure and compositions of the sintered pellets.

Room-temperature capacitance (C_p) and dielectric loss ($\tan\delta$) of the samples were measured with a parallel-plate capacitor arrangement using Agilent 4284A precision LCR meter from 10^2 to 10^6 Hz. Both sides of the samples were coated with silver-conducting paint to ensure good electrical contacts. The relative dielectric constant (ε_r) is determined from the relation $\varepsilon_r = dC_p/(\varepsilon_0 A)$, where ε_0 is the dielectric constant of vacuum, A is the cross-sectional area, d is the thickness of the sample.

3. Results and discussion

3.1. Subsolidus phase relationship in the ternary system $CuO–TiO_2–CaO$

The phase relationship in the ternary system $CuO–TiO_2–CaO$ sintered at 950 °C in air was tentatively determined by XRD measurements, as shown in Fig. 1. The investigated compositions are presented in Fig. 2. The phase relationship in this system can be divided into five bi-phasic regions of $CaCu_3Ti_4O_{12}$+$CaTiO_3$, $CaTiO_3$+CuO, CuO+$CaCu_3Ti_4O_{12}$, $CaTiO_3$+Ca_2CuO_3, $CaCu_3Ti_4O_{12}$+TiO_2 (see Fig. 1, lines ab, bd, da, bc, ae) and five tri-phasic regions of $CaCu_3Ti_4O_{12}$+$CaTiO_3$+CuO, $CaCu_3Ti_4O_{12}$+CuO+TiO_2, $CaCu_3Ti_4O_{12}$+TiO_2+$CaTiO_3$, $CaTiO_3$+CaO+Ca_2CuO_3, $CaTiO_3$+Ca_2CuO_3+CuO (see Fig. 1, regions I–V). The $CaCu_3Ti_4O_{12}$ compound is the only ternary oxide phase under these conditions in the investigated system.

Compared to the computed phase relations at 1000 °C [16], a disagreement existed about the number of possible compounds from $CaTiO_3$ to CaO. Though the CaO-rich compounds $Ca_3Ti_2O_7$ and $Ca_4Ti_3O_{10}$ were evaluated to be present at $1 \geq P_{O_2}/P^0 > 0.165$ [16,18], no experimental evidence was given so far. The powder diffraction patterns of $CaTiO_3$, $Ca_3Ti_2O_7$ and $Ca_4Ti_3O_{10}$ are very similar [13,19]. Nevertheless, their diffraction patterns can be distinguished in the X-ray diffractogram using diffractions below 30° (2θ) [19]. The most convincing evidences for the identification of $Ca_3Ti_2O_7$ and $Ca_4Ti_3O_{10}$ are the reflection at 18.2° (2θ) for $Ca_3Ti_2O_7$ and the diffraction line near 19.6° (2θ) for $Ca_4Ti_3O_{10}$ [13]. As we did not find any evidence for these lines in the diffraction diagrams and the lines of $CaTiO_3$ could be fully identified with respect to 2θ and the intensities, we can conclude that no

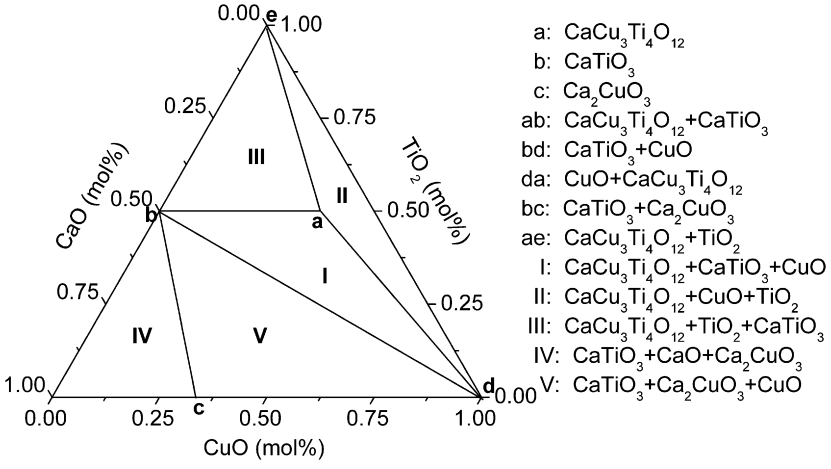

Fig. 1. Phase relationship in the ternary system $CuO–TiO_2–CaO$ at 950 °C in air. The phase relationship analysis is based on compositions shown in Fig. 2.

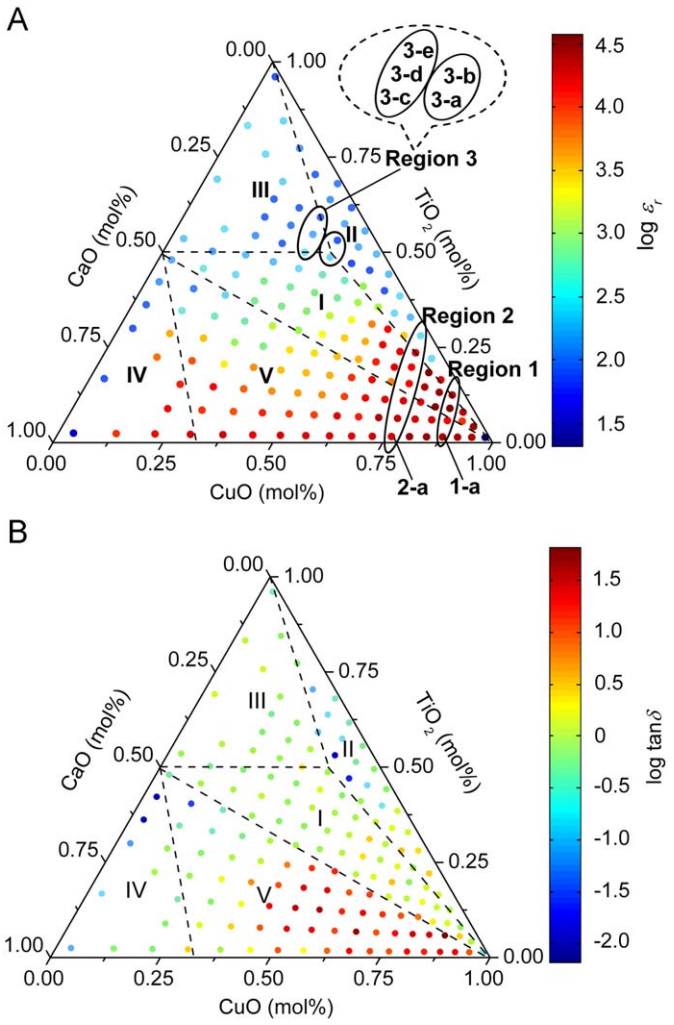

Fig. 2. Room temperature of (A) $\log \varepsilon_r$ and (B) $\log \tan \delta$ of the samples sintered at 950 °C in CuO–TiO_2–CaO system at 10 kHz. Colored dots represent the investigated compositions used to determine dielectric properties and the phase relations in Fig. 1. Dashed lines show the phase boundaries.

crystalline material of $Ca_3Ti_2O_7$ or $Ca_4Ti_3O_{10}$ is present in our samples (although there is one report stating that both compounds are stable at 950 °C) [18]. Calcium titanates are normally synthesized by solid-state reactions between $CaCO_3$ and TiO_2 at temperatures above 1300 °C [20]. The compound $Ca_3Ti_2O_7$ does not form readily at temperatures below 1480 °C [21]. The compound $Ca_4Ti_3O_{10}$ was reported to be the equilibrium product of the composition $4CaO \cdot 3TiO_2$, at least at 1650 °C [13]. This may explain why these compounds were not determined in the present study. Another possible explanation for the absence of $Ca_3Ti_2O_7$ and $Ca_4Ti_3O_{10}$ is that even longer sintering duration might be needed for their formation. At that point, we made no further investigations. Preliminary results show that in region V, the additional phase $CaCu_2O_3$ was also observed. The phase relation investigation in the system Ca–Cu–O showed that Ca_2CuO_3 was the only stable phase [9]. Roth et al. [10] reported that $CaCu_2O_3$ was stable between 985 and 1018 °C. In our study, a possible partial reaction between Ca_2CuO_3 and CuO might happen during the long-term sintering, and therefore produce a certain amount of $CaCu_2O_3$. Due to the complication in the subregion of $CaTiO_3$–CaO–CuO–$CaCu_3Ti_4O_{12}$ and the limited results, more detailed investigations in this region are required.

3.2. Dielectric property mapping in ternary system CuO–TiO_2–CaO

The room-temperature dielectric constant ε_r and loss $\tan \delta$ at 10 kHz in the ternary system CuO–TiO_2–CaO sintered at 950 °C are shown in Fig. 2. Most composites in CuO-rich region and along binary CuO–CaO line showed quite promising high ε_r ($>10^4$) (Fig. 2(A)). The ε_r of the composites in tri-phasic regions of II and III, both of which contain TiO_2, gave relatively low values. Compared to other phase regions, quite high values for $\tan \delta$ in the composites in phase region V were observed (Fig. 2(B)).

Sarkar et al. [5] reported that properly annealed CuO possesses giant ε_r. They proposed that using their route small portions of Cu^{3+} located at grain boundaries are responsible to get an electrically heterogeneous microstructure, containing semiconducting grains and insulating grain boundaries [22]. This is the desired electrical microstructure to produce the internal barrier layer effect, which is thought to be the most probable mechanism for giant dielectric constants. In our study, the particular microstructure of larger grains ($\approx 3\,\mu m$) of a predominant phase surrounded by smaller grains ($\approx 0.3\,\mu m$) of secondary phases were observed in the composites in the CuO-rich region and along CaO–CuO binary line. This microstructure seems to be important to explain the physical properties, which will be discussed in Section 3.3. Such types of microstructures probably follow the internal barrier layer capacitance effect to enhance the dielectric property of the composites.

Compared to the high dielectric constant of the composites in the CuO-rich region, the composites near $CaCu_3Ti_4O_{12}$ showed much lower $\varepsilon_r \approx 200$ when they were sintered at 950 °C. When treated at 1050 °C in air, quite high ε_r and great differences in microstructure were observed. The detailed data will be discussed in Section 3.4.

The combination of CuO–$CaCu_3Ti_4O_{12}$–$CaTiO_3$ was found to exist inside ternary system CuO–TiO_2–CaO. $CaTiO_3$ was used to produce dielectric composites due to its low $\tan \delta$[3]. $CaCu_3Ti_4O_{12}$ and CuO were both reported to show giant ε_r [1,5]. It seems to be very promising to investigate such combinations in detail in order to find the common characteristics in such high ε_r materials and to search for new composites with optimal dielectric properties. Further investigation of the detailed results and discussion concerning the correlation between the dielectric properties and phase distribution in ternary system CuO–$CaCu_3Ti_4O_{12}$–$CaTiO_3$ is underway.

3.3. Apparent correlation between dielectric property and phase distribution in CuO-rich region

In order to show the correlation between dielectric property and phase distribution in the CuO-rich region, composites of regions 1 and 2 (Fig. 2(A)) across the tri-phasic regions of V, I, II were chosen to demonstrate the frequency dependence of dielectric property in detail. Fig. 3 shows the frequency dependence of ε_r and $\tan \delta$ of representative samples (1-a)–(1-d) in region 1 and (2-a)–(2-g) in region 2 of Fig. 2(A). A clear difference of the dielectric behavior across different phase regions was observed. This is likely to depend on various characteristics such as different multiphase combinations and/or microstructures.

In phase region V, a relative plateau of ε_r ($>10^4$) was observed in samples (1-a) and (1-b) (Fig. 3(A)) and samples (2-a)–(2-c) (Fig. 3(B)) over the measured frequency range from 10^2 to10^6 Hz. In comparison, in phase region I, as seen in samples (1-c) and (1-d) (Fig. 3(A)) and samples (2-d)–(2-f) (Fig. 3(B)), ε_r slightly decreased with frequency increasing in the low-frequency range, while sharp decrease of ε_r in the high-frequency range was

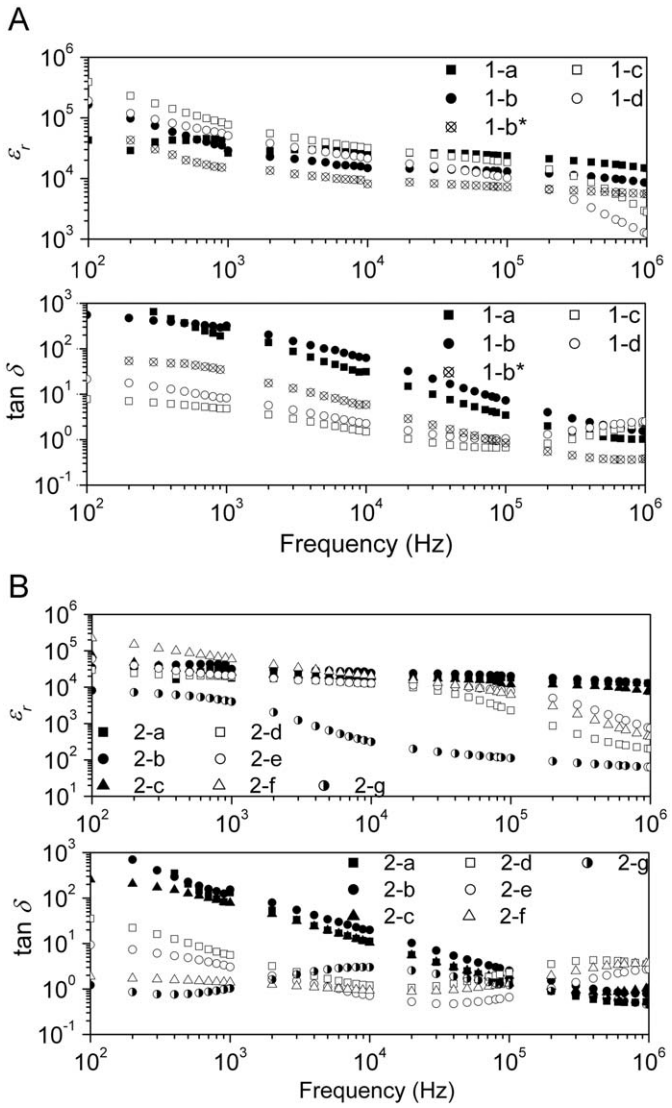

Fig. 3. The frequency dependence of ε_r (up) and tan δ (down) of (A): samples (1-a)–(1-d) (down to up) of region 1 and (B): samples (2-a)–(2-g) (down to up) of region 2 in Fig. 2(A). Sample (1-b*) has the same starting composition as sample (1-b), but sintered at 1000 °C, whereas others were sintered at 950 °C.

observed. The drastic drop of ε_r accompanied with a "loss peak" in the high-frequency range can be well described by a Debye-like relaxation [23]. The steep decrease in ε_r happens at the frequency where tan δ displays a relaxation peak. The relaxation peak occurred at 50 kHz for samples (2-d)–(2-f) (Fig. 3(B)), whereas it was found at around 100 kHz for samples (1-c) and (1-d) (Fig. 3(A)). When the TiO_2 phase exists in the composite, which is the case in phase region II, a drastic drop of ε_r behind 1 kHz accompanied with a broad loss peak was observed in sample (2-g) (Fig. 3(B)).

For the samples (1-a) and (1-b) (Figs. 2(a)) and (2-a)–(2-c) (Figs. 2(b)), extremely high tan δ were measured, especially at low frequencies. Such dielectric behavior was also observed in other composites along the CaO–CuO binary line. This implies a serious limitation to the application of such materials. The dc conductivity is possibly the main contribution to the high dielectric losses in such composites in phase region V.

The dielectric loss of ceramic materials is also influenced by the extrinsic loss arising from porosity, secondary phases, grain size and defects, etc. induced by processing [24]. For example, when higher sintering temperature (1000 °C instead of 950 °C) was applied in the same composition as sample (1-b), a large decrease of tan δ and a slight decrease of ε_r were observed (sample (1-b*) in Fig. 3(A)). This might be caused by the densification of the sample and by the decrease of porosity after sintering at higher temperature. Fig. 4 shows the microstructure of these two samples. A bimodal grain size distribution was observed. The bigger grains were found to be composed of only copper oxide by EDX analysis. The smaller grains with the secondary phases were situated on the bigger copper oxide grains. Compared to (1-b), sample (1-b*) shows the growing of both types of grains. The porosity of the sample (1-b*) treated at 1000 °C is much lower than (1-b) at 950 °C (Fig. 4). These preliminary results show that a

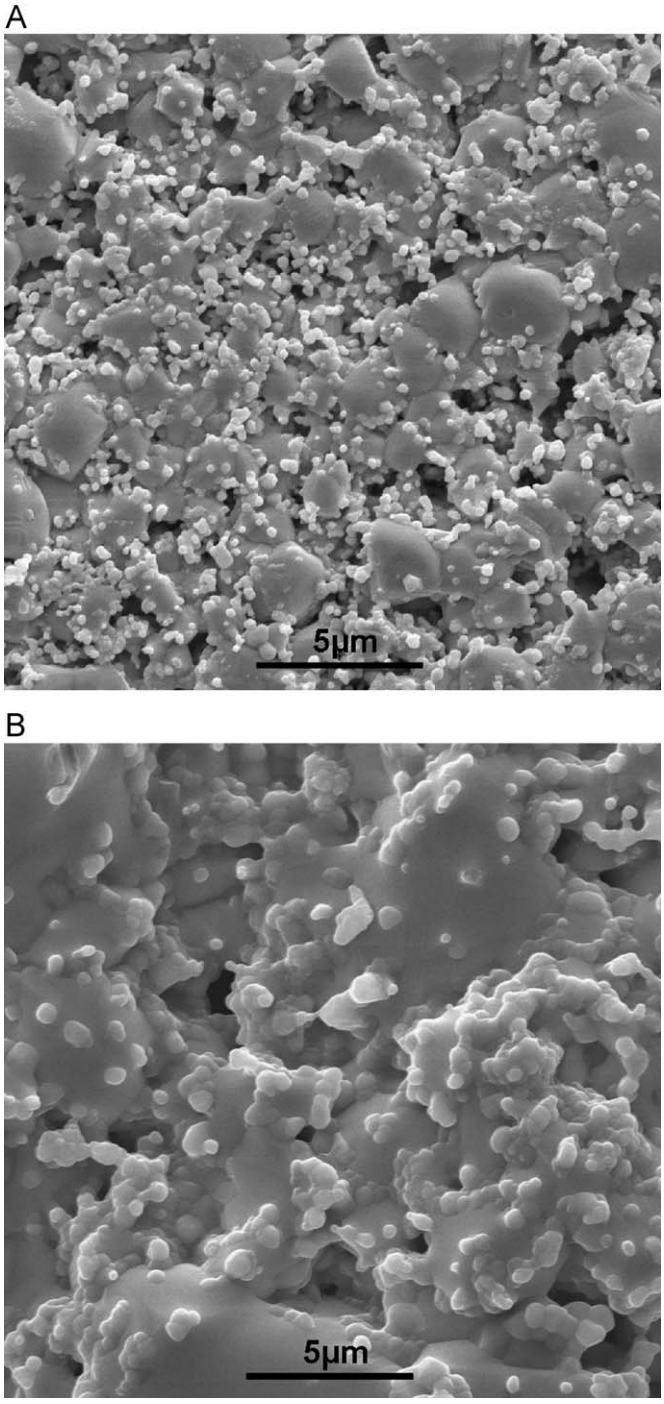

Fig. 4. SEM images of (A): sample (1-b) and (B): sample (1-b*) in Fig. 3 with sintering temperature of 950 and 1000 °C, respectively.

decrease of the dielectric loss by sintering at higher temperature may be triggered. Due to the limitation of the liquidus temperature, the sintering temperature was kept below 1000 °C. Therefore, further optimization of the process in view of the decrease of tan δ may be probably studied by "soft chemistry" method, in which the temperature for sintering would be much lower compared to solid-state reaction.

The typical bimodal grain size distribution observed in SEM, such as sample (1-b), was also found in some of the other samples along the CaO–CuO binary line (not shown). The bigger grains with predominant phase were found in a fine-grained matrix of secondary phases.

3.4. The dielectric properties in $CaCu_3Ti_4O_{12}$-rich region

Considerable interest to $CaCu_3Ti_4O_{12}$ has been stimulated since $CaCu_3Ti_4O_{12}$ was observed to show giant ε_r by Subramanian [1]. Furthermore, $CaCu_3Ti_4O_{12}$ has been reported to have quite different values of the dielectric constant because of different microstructures in the ceramic samples [25]. Fang et al. [25] observed that ε_r of $CaCu_3Ti_4O_{12}$ becomes higher than 10^4 only when there are large grains (10–20 μm) in the sintered ceramic samples. Adams et al. [6] achieved $\varepsilon_r >$ in large-grain ($\approx$100 μm) $CaCu_3Ti_4O_{12}$ ceramics, which is 2 orders of magnitude higher than fine-grained ($\approx$5 μm) $CaCu_3Ti_4O_{12}$ ceramic. They argued that large grains may be crucial for enhancement of the dielectric constant. Liu et al. [4] found that $CaCu_3Ti_4O_{12}$ exhibits $\varepsilon_r \approx 10^4$ with small grain sizes (2–3 μm). They believe that the density of the sample is the key factor for the large dielectric constant in their samples prepared by a sol–gel process [4].

Due to a possible liquidus temperature in CuO-rich region, the samples near CuO cannot be treated higher than 1000 °C; some of them partially melted even below 1000 °C. Herein, 950 °C was chosen as the sintering temperature for the dielectric property mapping in ternary system CuO–TiO_2–CaO. The composites in $CaCu_3Ti_4O_{12}$-rich region sintered at 950 °C exhibit $\varepsilon_r \approx 200$ at 10 kHz, as can be seen in Fig. 2(A). When the composites in $CaCu_3Ti_4O_{12}$-rich region were sintered at 1050 °C, quite different dielectric behavior was observed.

Fig. 5 presents the dielectric constant and dielectric loss dependence on frequency at room temperature for $CaCu_3Ti_4O_{12}$-rich samples (3-a)–(3-e) in region 3 of Fig. 2(A) sintered at 1050 °C. A weak dependence of ε_r on frequency was observed in these samples. The highest ε_r ($\approx 10^4$) was observed in sample (3-a), which is the $CaCu_3Ti_4O_{12}$-richest sample in this library. Samples (3-c)–(3-e) also exhibited quite high ε_r, though slightly lower than that of sample (3-a). Sample (3-b) gave the lowest ε_r compared with other samples treated at 1050 °C, but still remained impressively high ε_r ($>10^3$ below 30 kHz). The corresponding X-ray diffraction patterns for the investigated samples sintered at 1050 °C are given in Fig. 6. Samples (3-c) and (3-e) are bi-phasic composites of ($CaCu_3Ti_4O_{12}$+$CaTiO_3$) and ($CaCu_3Ti_4O_{12}$+TiO_2), respectively. Sample (3-d) is a composite of three phases ($CaCu_3Ti_4O_{12}$+$CaTiO_3$+TiO_2). These composites exhibit very high ε_r with low dielectric loss when sintered at 1050 °C (Fig. 5), in comparison to those sintered at 950 °C. Microstructure evolution and different phase combination in such composites seem to play an important role for enhancement of the dielectric properties. The influence of phase distribution on the dielectric property in such a region is unclear yet, and needs more systematic investigations.

Sample (3-a) is the $CaCu_3Ti_4O_{12}$-richest sample in this library with minor secondary phases of $CaTiO_3$ and Cu_2O (Fig. 6). Comparing to sample (3-a*) sintered at 950 °C, which has the same starting composition as sample (3-a), much higher ε_r and lower tan δ were observed in sample (3-a), as seen from Fig. 5. The microstructures of these two samples were investigated by SEM (Fig. 7). In sample (3-a*) (Fig. 7(A)), the grains are homogeneous in shape and size, approximately ranging from 0.5 to 2 μm. In comparison, sample (3-a) treated at 1050 °C shows a quite different microstructure, as seen from Fig. 7(B). Two types of grains were observed. There are bigger grains with grain sizes of approximately 10–30 μm and there are smaller grains with grain sizes $\approx$2 μm located at the triple point of the bigger grains or the grain boundaries. Additionally, a liquid phase was found on the grain boundaries. EDX analysis reveals different compositions in the big grains, the small grains and the liquid phase (see Fig. 7(B)). $CaCu_3Ti_4O_{12}$, $CaTiO_3$ and copper oxide (either CuO or Cu_2O) have been thus localized, respectively. CuO will decompose into Cu_2O at temperature above 1000 °C in air [26]. It may be assumed that copper oxide transforms into a liquid phase during the sintering treatment and leads to anomalous grain growth. The existence of $CaTiO_3$ and a copper oxide wetting layer might be considered as

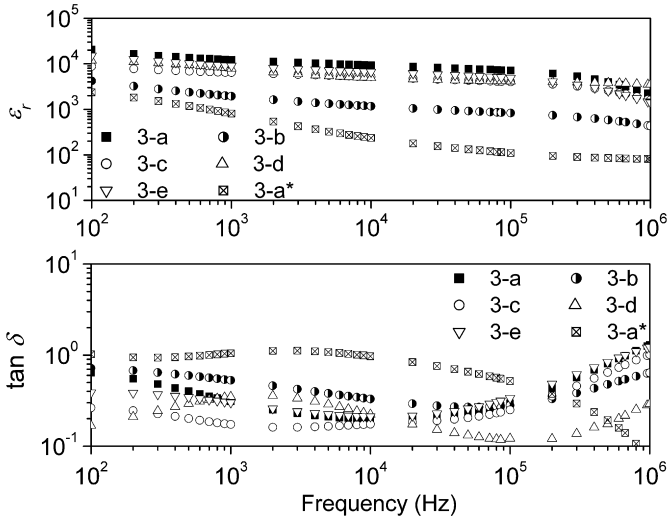

Fig. 5. The frequency dependence of ε_r (up) and tan δ (down) of samples (3-a)–(3-e) in region 3 of Fig. 2(A). Sample (3-a*) has the same starting composition as sample (3-a), but sintered at 950 °C, whereas others were sintered at 1050 °C.

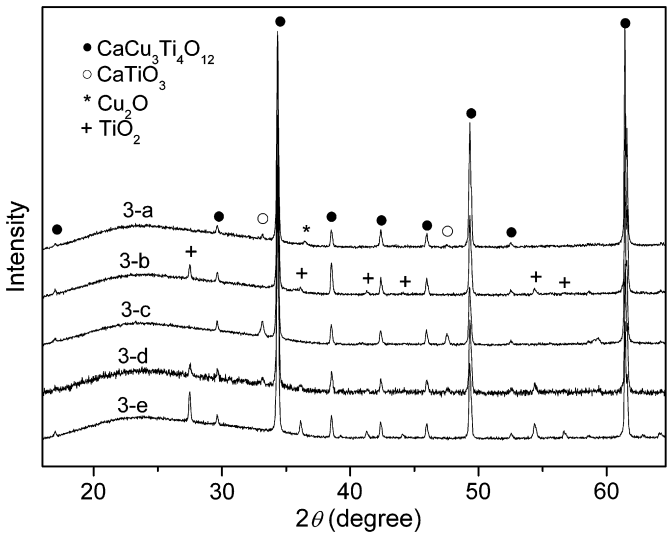

Fig. 6. X-ray diffraction patterns of samples (3-a)–(3-e) in region 3 of Fig. 2(A), sintered at 1050 °C.

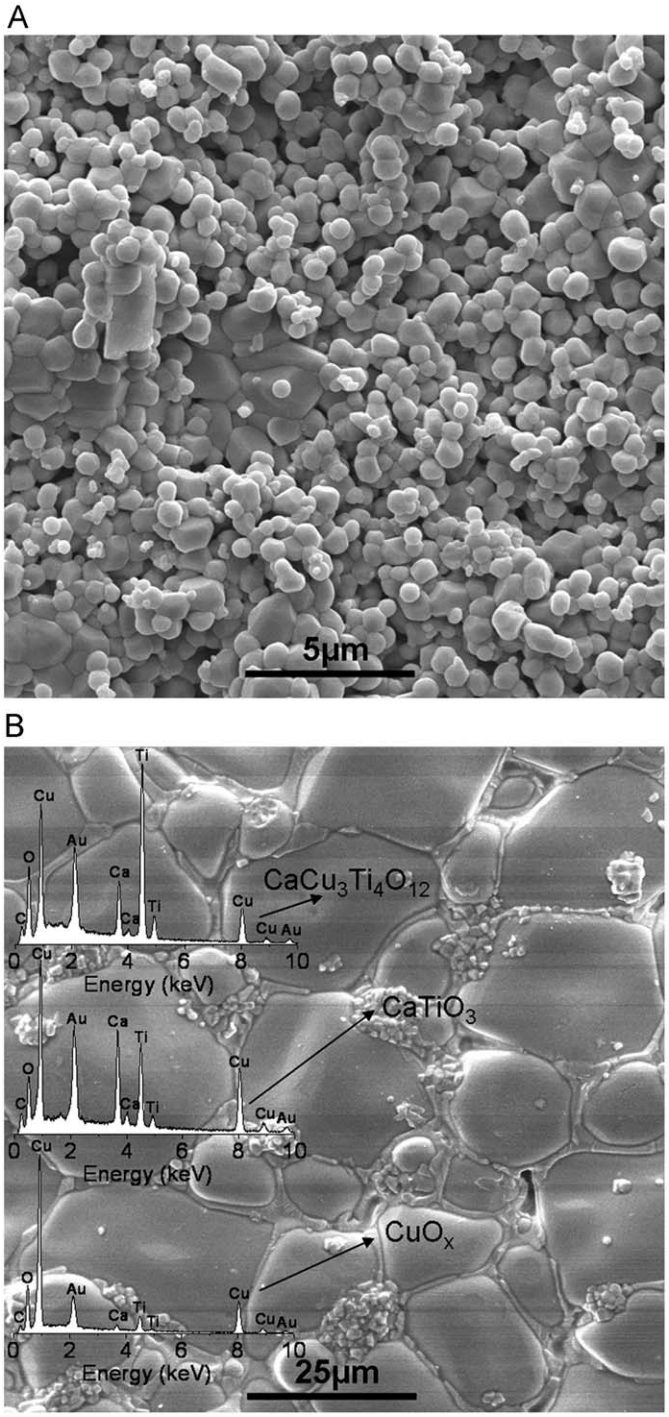

Fig. 7. SEM micrographs of (A): sample (3-a*) and (B): sample (3-a) in Fig. 5 sintered at 950 and 1050 °C, respectively. Insets in (B) show the composition analysis by EDX for big grain (up), small grains (middle), and liquid phase (down), respectively.

the barrier layers of the $CaCu_3Ti_4O_{12}$ grains promoting the dielectric property of $CaCu_3Ti_4O_{12}$.

The origin of the peculiar dielectric phenomena is not fully understood so far. In our study, the clear grain-boundary effect was observed in the high dielectric constant materials both in CuO-rich region sintered at 950 °C and in $CaCu_3Ti_4O_{12}$-rich region sintered at 1050 °C. This supports a model with an extrinsic internal barrier layer capacitance mechanism coming from grain-boundary effect. However, giant dielectric constants were also reported in a single-crystal $CaCu_3Ti_4O_{12}$. It was proposed that the locally planar twin boundary and the antiphase and compositional ordering domain boundaries act as the barrier layers in the single crystal since a perfectly grown single crystal of $CaCu_3Ti_4O_{12}$ shows only a dielectric constant of 100 [27]. Fang et al. [27] observed that the different domains existed inside the grains and suggested both domain boundaries and grain boundaries acting as the barrier layers to contribute to the extraordinary dielectric response in $CaCu_3Ti_4O_{12}$. The discovery of internal domains inside the grains correlates the dielectric mechanism for both polycrystalline and single-crystal materials. The domain boundaries might also exist in our composites, which needs further confirmation.

4. Conclusion

Subsolidus phase relationship and dielectric properties in the ternary system $CuO–TiO_2–CaO$ were studied. Five bi-phasic regions and five tri-phasic regions and only one ternary compound $CaCu_3Ti_4O_{12}$ were found in this system.

Giant dielectric constants were found in two regions in the ternary system $CuO–TiO_2–CaO$: One is the CuO-rich region and along the CaO–CuO binary line, in which the composites possess ε_r over 10^4. This composite can be fabricated in a single step at a low sintering temperature of 950 °C. The other is the $CaCu_3Ti_4O_{12}$-rich region sintered at 1050 °C. A quite high $\tan\delta$ was observed in composites in the phase region of ($CuO+CaTiO_3+Ca_2CuO_3$). The low resistivity and Debye relaxation might be two main contributions to the high dielectric loss.

The grain size distributions in most of the giant ε_r composites are found to be bimodal. Smaller grains with secondary phases are located on the surface or the boundaries of the bigger grains, which are composed of the predominant phases. The smaller grains might act as barrier layers and might enhance the dielectric property. The composites in the $CaCu_3Ti_4O_{12}$-rich region show a clear grain-boundary effect made of presumably liquidus copper oxide and/or $CaTiO_3$.

It is currently premature, to associate the special microstructures and phase distributions with the promising dielectric properties of the composites in the ternary system $CuO–TiO_2–CaO$. More investigations such as the temperature dependence of dielectric properties in the representative composites with giant ε_r will be explored in the future.

Acknowledgments

The authors would like to acknowledge useful discussions with Dr. M. Aslan and Dr. M. Quilitz.

References

[1] M.A. Subramanian, D. Li, N. Duan, B.A. Reisner, A.W. Sleight, J. Solid State Chem. 151 (2000) 323–325.
[2] C.C. Homes, T. Vogt, S.M. Shapiro, S. Wakimoto, A.P. Ramirez, Science 293 (2001) 673–676.
[3] W. Kobayashi, I. Terasaki, Appl. Phys. Lett. 87 (2005) 032902.
[4] J. Liu, Y. Sui, C. Duan, W. Mei, R.W. Smith, J.R. Hardy, Chem. Mater. 18 (2006) 3878–3882.
[5] S. Sarkar, P.K. Jana, B.K. Chaudhuri, Appl. Phys. Lett. 89 (2006) 212905.
[6] T.B. Adams, D.C. Sinclair, A.R. West, Adv. Mater. 14 (2002) 1321–1323.
[7] D. Capsoni, M. Bini, V. Massarotti, G. Chiodelli, M.C. Mozzatic, C.B. Azzoni, J. Solid State Chem. 177 (2004) 4494–4500.
[8] W.Y. Wang, D.F. Zhang, X.L. Chen, J. Mater. Sci. 38 (2003) 2049–2054.
[9] T. Mathews, J.P. Hajra, K.T. Jacob, Chem. Mater. 5 (1993) 1669–1675.
[10] R.S. Roth, N.M. Hwang, C.J. Rawn, B.P. Burton, J.J. Ritter, J. Am. Ceram. Soc. 74 (1991) 2148–2151.
[11] N. Kobayashi, Z. Hiroi, M. Takano, J. Solid State Chem. 132 (1997) 274–283.
[12] R.C. Devries, R Roy, E.F. Osborn, J. Phys. Chem. 58 (1954) 1069–1073.
[13] R.S. Roth, J. Res. NBS 61 (1958) 437–440.

[14] D. Hennings, J. Solid State Chem. 31 (1980) 275–279.
[15] F.-H. Lu, F.-X. Fang, Y.-S. Chen, J. Eur. Ceram. Soc. 21 (2001) 1093–1099.
[16] K.T. Jacob, C. Shekhar, X. Li, G.M. Kale, Acta Mater. 56 (2008) 4798–4803.
[17] S. Ren, W. Kochanek, H. Bolz, M. Wittmar, I. Grobelsek, M. Veith, J. Eur. Ceram. Soc. 28 (2008) 3005–3010.
[18] K.T. Jacob, K.P. Abraham, J. Chem. Thermodyn. 41 (2009) 816–820.
[19] M. Ceh, D. Kolar, J. Mater. Sci. 29 (1994) 6295–6300.
[20] G. Pfaff, Chem. Mater. 6 (1994) 58–62.
[21] W. Kwestroo, H.A.M. Paping, J. Am. Ceram. Soc. 42 (1959) 292–299.
[22] S. Sarkar, P.K. Jana, B.K. Chaudhuri, Appl. Phys. Lett. 92 (2008) 022905.
[23] K.S. Cole, R.H. Cole, J. Chem. Phys. 9 (1941) 341–351.
[24] X. Kuang, M.M.B. Allix, J.B. Claridge, H.J. Niu, M.J. Rosseinsky, R.M. Ibberson, D.M. Iddles, J. Mater. Chem. 16 (2006) 1038–1045.
[25] T.T. Fang, H.K. Shiau, J. Am. Ceram. Soc. 87 (2004) 2072–2079.
[26] S. Guillemet-Fritsch, T. Lebey, M. Boulos, B. Durand, J. Eur. Ceram. Soc. 26 (2006) 1245–1257.
[27] T.T. Fang, C.P. Liu, Chem. Mater. 17 (2005) 5167–5171.